NEOPLASIA
www.neoplasia.com

Volume 18 Number 3 March 2016 pp. 133–141 133

Visualization of the Biological Behavior of Tumor-Associated Macrophages in Living Mice with Colon Cancer Using Multimodal Optical Reporter Gene Imaging

Yun Ju Choi*,1, Seul-Gi Oh*,1, Thoudam Debraj Singh*, Jeoung-Hee Ha†, Dong Wook Kim§, Sang Woo Lee*, Shin Young Jeong*, Byeong-Cheol Ahn*, Jaetae Lee*,‡ and Young Hyun Jeon*,§

*Department of Nuclear Medicine, Kyungpook National University, Daegu, Korea; †Department of Pharmacology, Kyungpook National University, Daegu, Korea
‡Daegu-Gyeongbuk Medical Innovation Foundation (DGMIF), Daegu, Korea; §Leading-edge Research Center for Drug Discovery and Development for Diabetes and Metabolic Disease, Kyungpook National University Hospital, Daegu, Korea

Abstract

We sought to visualize the migration of tumor-associated macrophages (TAMs) to tumor lesions and to evaluate the effects of anti-inflammatory drugs on TAM-modulated tumor progression in mice with colon cancer using a multimodal optical reporter gene system. Murine macrophage Raw264.7 cells expressing an enhanced firefly luciferase (Raw/effluc) and murine colon cancer CT26 cells coexpressing Rluc and mCherry (CT26/Rluc-mCherry, CT26/RM) were established. CT26/RM tumor-bearing mice received Raw/effluc via their tail veins, and combination of bioluminescence imaging (BLI) and fluorescence imaging (FLI) was conducted for *in vivo* imaging of TAMs migration and tumor progression. Dexamethasone (DEX), a potent anti-inflammatory drug, was administered intraperitoneally to tumor-bearing mice following the intravenous transfer of Raw/effluc cells. The migration of TAMs and tumor growth was monitored by serial FLI and BLI. The migration of Raw/effluc cells to tumor lesions was observed at day 1, and BLI signals were still distinct at tumor lesions on day 4. Localization of BLI signals from migrated Raw/effluc cells corresponded to that of FLI signals from CT26/RM tumors. *In vivo* FLI of tumors demonstrated enhanced tumor growth associated with macrophage migration to tumor lesions. Treatment with DEX inhibited the influx of Raw/effluc cells to tumor lesions and abolished the enhanced tumor growth associated with macrophage migration. These findings suggest that molecular imaging approach for TAM tracking is a valuable tool for evaluating the role of TAMs in the tumor microenvironment as well as for the development of new drugs to control TAM involvement in the modulation of tumor progression.

Neoplasia (2016) 18, 133–141

Introduction

Macrophages are important immune cells involved in the onset, progression, and manifestation of various pathologic processes, such as the development of malignant tumors and various inflammatory diseases [1–4]. They are divided into classically activated macrophages (M1) and alternatively activated macrophages (M2 or tumor-associated macrophages, TAMs). M1 macrophages are activated by interferon-γ, tumor necrosis factor–α, or lipopolysaccharides; they have immunostimulatory properties and generate a Th1 immune response. Contrary to M1 macrophages, M2 macrophages with poor antigen-presenting capacity suppress Th1 adaptive immunity [5].

Recently, several studies have demonstrated that TAMs not only facilitate tumor angiogenesis, extracellular matrix degradation, and remodeling but also promote tumor cell motility [6,7]. Furthermore, direct communication between TAMs and cancer cells results in the invasion of tumor cells into blood vessels. TAMs are found in the center of the tumor microenvironment and are important targets for

Address all correspondence to: Jaetae Lee, M.D., Ph.D., Department of Nuclear Medicine, Kyungpook National University Hospital, 50 Samduk 2-ga, Daegu 700-721, South Korea. or Yong Hyun Jeon, Ph.D., Leading-edge Research Center for Drug Discovery and Development for Diabetes and Metabolic Disease, Kyungpook National University Hospital, 807 Hogukro, Bukgu, Daegu 702-210, South Korea.
E-mail: jaetae@knu.ac.kr

[1] Contributed equally to this study.

Received 22 September 2015; Revised 5 January 2016; Accepted 12 January 2016

1476-5586
http://dx.doi.org/10.1016/j.neo.2016.01.004

cancer therapy [8]; accordingly, many studies have examined the biological role of TAMs in cancer and have identified promising therapeutic drugs to modulate their involvement in tumor progression. However, analyses of the complex biological, pathological, and immunological factors involved in the relationship between TAMs and tumor-bearing hosts are still limited. Therefore, robust and quantitative techniques are necessary to assess the dynamic functions of TAMs in tumor microenvironments.

Molecular-genetic imaging strategies are based on a reporter gene and a complementary reporter probe, which are introduced into cells to visualize proliferation, localization, and migration in living subjects [9,10]. Among several reporter gene-based imaging modalities, optical imaging with bioluminescent or fluorescent reporter genes is widely used and is useful for cell tracking and for the evaluation of therapeutic outcomes in various preclinical models owing to their high sensitivity, simple imaging procedures, and no requirement of complex imaging facilities, such as positron emission tomography, single-photon emission computed tomography, and magnetic resonance imaging (MRI) systems.

In this study, we attempted to demonstrate TAM migration to tumor lesions using an enhanced firefly luciferase in living mice with colon cancer. To accomplish this study, we used Raw264 macrophage cells with characteristics of TAM for optical imaging of the TAM kinetics. Furthermore, Renilla luciferase (Rluc) and mCherry reporter genes were introduced to monitor the proliferation of colon cancer cells in response to TAMs *in vitro* and *in vivo*. Finally, the effects of dexamethasone (DEX, an anti-inflammatory drug) on the migration of TAMs to tumor lesions as well as on the TAM-mediated modulation of tumor progression were evaluated using the established multimodal reporter imaging strategies.

Materials and Methods

Animals

Pathogen-free 6-week-old female BALB/c mice were obtained from SLC Inc. (Shizuoka, Japan). All animal experimental protocols were approved by the Committee for the Handling and Use of Animals at Kyungpook National University.

Cells

Murine macrophage Raw264.7 cells were cultured in Dulbecco's modified Eagle medium supplemented with 10% fetal bovine serum and 1% antibiotic-antimycotic (Invitrogen, Carlsbad, CA) at 37°C in a 5% CO_2 atmosphere. Raw264.7 cells were retrovirally transduced to express both effluc and Thy1.1. The Thy1.1-positive cells were sorted using CD90.1 MicroBeads (Miltenyi Biotec, Auburn, CA). The established stable macrophage cells expressing both effluc and Thy1.1 are herein named as Raw/effluc cells.

The murine colon cancer cell line CT26 was transduced with a lentivirus coexpressing the Rluc and mCherry genes (GeneCopoeia Inc., Rockville, MD). Two days later, mCherry-positive cells were enriched using the FACS Aria III (BD Biosciences, San Jose, CA). The stable clones coexpressing Rluc and mCherry are named as CT26/RM cells.

For the luciferase assay, the indicated numbers of parental and reporter cells were plated in 96-well Black Plates with clear bottoms. After 24 hours, each well was supplemented with either D-luciferin (DV Medical Research Innovations, Adrian, MI) or coelenterazine h (NanoLight, AZ, USA). Bioluminescence imaging (BLI) signals were measured using an IVIS Lumina III imaging system (PerkinElmer, Waltham, MA).

Cellular Proliferation Assay

For the *in vitro* analysis, CT26/RM cells (1×10^4 cells/well) were plated without or with Raw/effluc cells (1×10^3 cells/well). After 24 hours, BLI activity was measured with an IVIS Lumina III, and fluorescence imaging (FLI) was acquired with a fluorescent microscope.

For the *in vivo* analysis, CT26/RM cells (1×10^6 cells) were mixed without or with Raw/effluc cells (1×10^5 cells), and these mixtures were subcutaneously injected to predetermined sites in the mice. *In vivo* proliferation rates of CT26/RM cells were determined by BLI at days 1, 2, and 6 postinjection.

Transwell Migration Assay

To prepare conditioned medium (CM), CT26/RM cells were grown to 70% to 80% confluence in completed culture media. The medium was replaced with serum-free RPMI-1640, and cells were cultured for an additional 48 hours. Raw/effluc cells were resuspended in serum-free RPMI-1640 and cultured for 48 hours. Medium was collected and filtered with 0.22-μm filters (Millipore, Billerica, MA). The 8-μm pore Transwell polycarbonate membrane chambers (Corning, Pittston, PA) were used. Raw/effluc cells (1×10^5) in 100 μl of serum-free medium (SFM) were added to the upper chamber. CM from CT26/RM was added to the lower chamber. The cells were allowed to migrate through the membrane for 24 hours at 37°C in a 5% CO_2 atmosphere. The cells that migrated to the bottom chamber were collected and counted by flow cytometry. Events acquired over a fixed time period (60 seconds) were analyzed using FlowJo analysis software.

In Vivo Study

Study 1. For *in vivo* tracking of TAMs, CT26/RM was subcutaneously administered to mice. CT26/RM tumor-bearing mice were divided into two groups: CT26/RM and CT26/RM + Raw/effluc. Either phosphate-buffered saline (PBS) or Raw/effluc cells (5×10^6 in 0.1 ml of PBS) was intravenously transferred to tumor-bearing mice. BLI (for TAM imaging) was conducted once daily from day 1 to until day 4 posttransfer of Raw/effluc cells. For tumor imaging, *in vivo* FLI with filter settings for mCherry using the IVIS Lumina III was performed at the indicated times posttransfer of macrophages.

Study 2. To evaluate the effect of DEX (Sigma, St. Louis, MO) on both TAMs migration as well as on TAMs modulation of tumor growth, CT26/RM tumor-bearing mice were divided into three groups: CT26/RM, CT26/RM+Raw/effluc, and CT26/RM+Raw/effluc+DEX. Mice received 10 mg/kg DEX immediately via intraperitoneal injection following the transfer of Raw/effluc cells. Daily treatment with DEX was sustained for 3 days. *In vivo* BLI and FLI were performed at the indicated times.

For *in vivo* BLI, mice received either D-luciferin (for effluc) or coelenterazine h (for Rluc) via either intraperitoneal or intravenous injection. BLI was performed at 10 minutes (effluc) or immediately (Rluc) after the injection of the respective substrate using the IVIS Lumina III imaging system (PerkinElmer). Grayscale photographic images and bioluminescent color images were superimposed using LIVINGIMAGE (version 2.12, PerkinElmer) and IGOR Image Analysis FX software (WaveMetrics, Lake Oswego, OR). BLI signals are expressed in units of photons per cm^2 per second per steradian ($P/cm^2/s/sr$). All mice were anesthetized using 1% to 2% isoflurane gas during imaging.

Ex Vivo and FACS Analysis

For *ex vivo* imaging of the specimen, mice were sacrificed and tumors were excised. The excised tumors were placed on an imaging plate, and images were acquired.

On day 4 posttransfer of Raw/effluc cells, the excised tumors were incubated with tumor dissociation solution including collagenase D solution and DNase I to isolate single suspended cells. These cells were washed with cold PBS twice and labeled with APC-Cy7–conjugated Thy1.1 antibody (BD Biosciences). The percentage of Thy1.1-positive cells was determined with flow cytometry (BD ACCURI C6; BD Biosciences).

Statistical Analysis

All data are expressed as means ± standard deviation from at least three representative experiments, and statistical significance was determined using an unpaired Student's *t* test. *P* values less than .05 were considered statistically significant.

Results

Reporter Gene Expression and Its Functional Activity in Raw/effluc and CT26/RM Cells

Flow cytometric analysis demonstrated higher levels of effluc and mCherry expression in both Raw/effluc and CT26/RM cells (Figure 1*A*). Levels of effluc and mCherry expression in Raw/effluc and CT26/RM cells were 93% and 87.2%, respectively. Fluorescent microscopy revealed bright signals of the mCherry protein in CT26/RM cells (Supplementary Figure 1*A*). The mCherry gene is coexpressed with Rluc by the IRES system in CT26/RM cells; accordingly, similar Rluc expression levels can be inferred, i.e., approximately 87.2%. An immunoblotting analysis with an Rluc-specific antibody indicated Rluc expression in CT26/RM cells but not in parental CT26 cells (Supplementary Figure 1*B*).

In vitro BLI of Raw/effluc and CT26/RM cells revealed the cell number–dependent increase in luciferase signals; there was a strong correlation between cell number and BLI signals (Figure 1, *B* and *C*) (R^2 = 0.89 and 0.95 for Raw/effluc and CT26/RM cells, respectively). However, no signals were detected in the parental cells. As illustrated in Figure 1*D*, distinct FLI signals were detected in CT26/RM tumors, and the presence of directly injected Raw/effluc cells at the tumor site was confirmed by BLI.

Enhanced Proliferation of Colon Cancer Cells by TAMs and Increased Migration Ability by CM of CT26/RM

In vitro BLI with Rluc demonstrated higher proliferation of CT26/RM+Raw/effluc cells than in those with CT26/RM alone. Consistent with *in vivo* BLI, fluorescent microscope imaging revealed an increased number of cancer cells in CT26/RM+Raw/effluc cells compared with CT26/RM alone (Figure 2, *A* and *B*). Rluc activity was

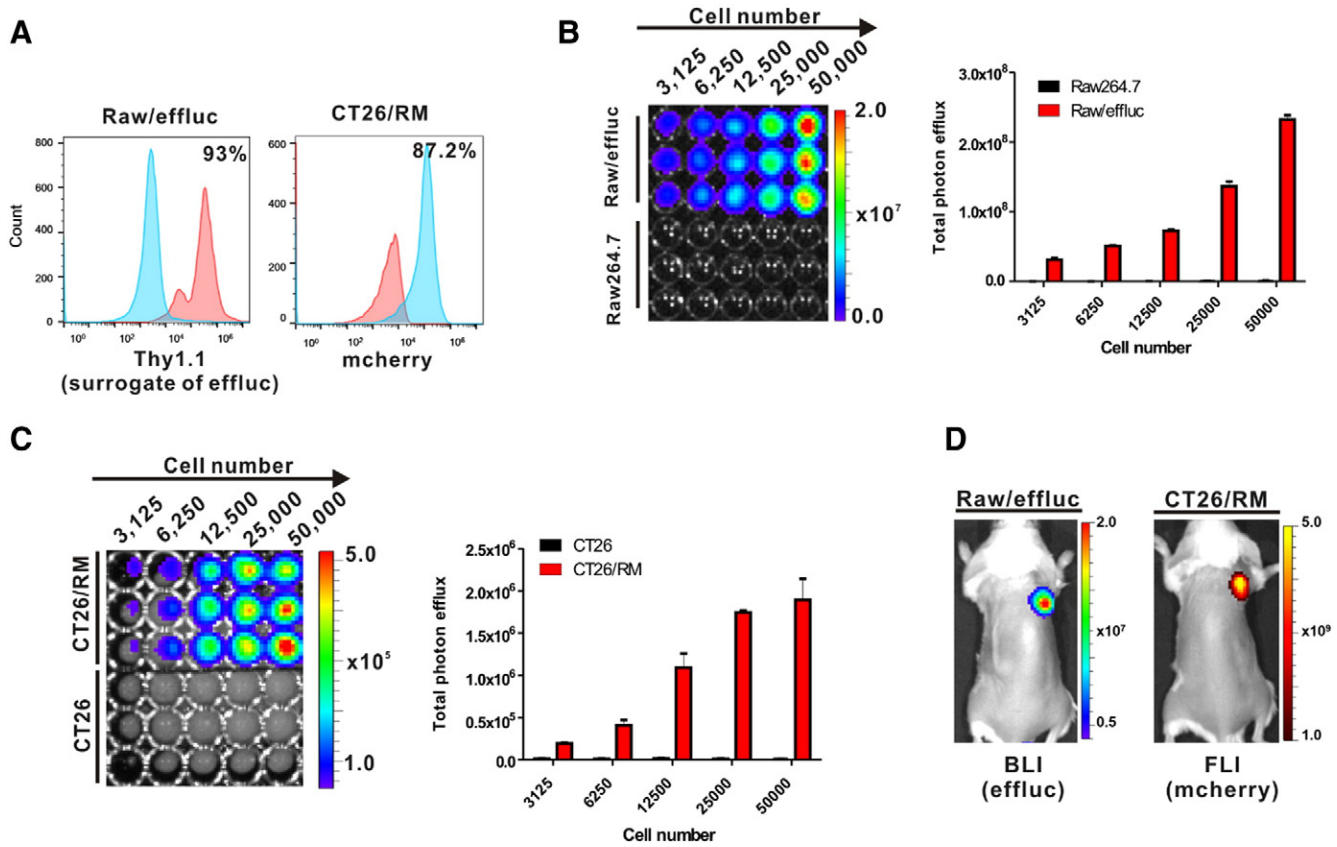

Figure 1. Tumor-associated macrophages and colon cancer cells expressing optical reporter genes. (A) FACS analysis of Raw/effluc cells. Left: Raw/effluc cells indicate cells labeled with either isotype (blue) or Thy1.1-specific antibody (red). Right: Parental CT26 (blue) and stable CT26/RM cells (RED). (B) *In vitro* BLI of either parental Raw264.7 or Raw/effluc cells and quantification of BLI signal. (C) *In vitro* BLI of either parental CT26 cells or CT26/RM cells (left) and quantification of BLI signal (right). (D) Imaging of TAMs and colon cancer models with either effluc or Rluc. Tumor-bearing mice received Raw/effluc cells intratumorally, and then FLI and BLI were conducted.

$1.29 \times 10^6 \pm 1.16 \times 10^5$ and $3.73 \times 10^6 \pm 5.49 \times 10^5$ P/cm^2/s/sr in CT26/RM-alone and CT26/RM+Raw/effluc cells, respectively ($P < .05$).

The migration levels of Raw/effluc cells were higher in CM of CT26/RM cells than in SFM (Figure 2*C*). The migration levels of Raw/effluc cells increased in a dose-dependent manner for CM derived from CT26/RM cells.

Next, we examined whether Raw/effluc cells enhance the proliferation of CT26/RM cells *in vivo*. As shown in Figure 2*D*, no significant difference of proliferation levels was observed between CT26/RM+Raw/effluc cells and CT26/RM alone from day 0 postinoculation. However, enhanced proliferation of cancer cells was distinct at coinjection sites at day 7 postinoculation ($P < .05$).

In Vivo Imaging of TAM Migration to Tumor Lesions

We serially tracked TAM migration to tumor lesions by combined BLI and FLI (Supplementary Figure 2*A*). As illustrated in Figure 3, *A* and *B*, BLI with effluc showed the early distribution of infused Raw/effluc cells to the lung within 30 minutes posttransfer. Interestingly, BLI signals from Raw/effluc cells were detected in tumor lesions as early as day 1 after the transfer of Raw/effluc cells (see red arrow in Figure 3). Their migration to tumor lesions was still detected at day 4 posttransfer of Raw/effluc cells despite fluctuation in the BLI signal of Raw/effluc cells in tumor lesions. The BLI signal emitted from migrated Raw/effluc cells corresponded well to the FLI signal from CT26/RM tumors.

Tumors were excised to further validate the localization of migrated TAMs by *ex vivo* imaging at day 4 posttransfer of Raw/effluc cells. A distinct BLI signal from Raw/effluc cells was also observed in excised tumors by *ex vivo* BLI (Figure 3*A*, *inset*). Furthermore, FACS analysis with a Thy1.1-specific antibody confirmed the existence of Raw/effluc cells in excised CT26/RM tumors and showed that levels of Thy1.1-positive cells ranged from 3.9% to 14.3% (Figure 3, *C* and *D*). However, we cannot see the increase of Thy1.1-positive cells in excised tumors from mice inoculated with CT26/RM only (Supplementary Figure 2*B*).

In Vivo FLI of Enhanced Tumor Growth via Migrated Raw/effluc Cells

We evaluated the effects of the presence of migrated TAMs on tumor progression by serially monitoring FLI signals (Supplementary Figure 3). There was no significant difference between the CT26/RM-alone group and the CT26/RM+Raw/effluc group at day 0,

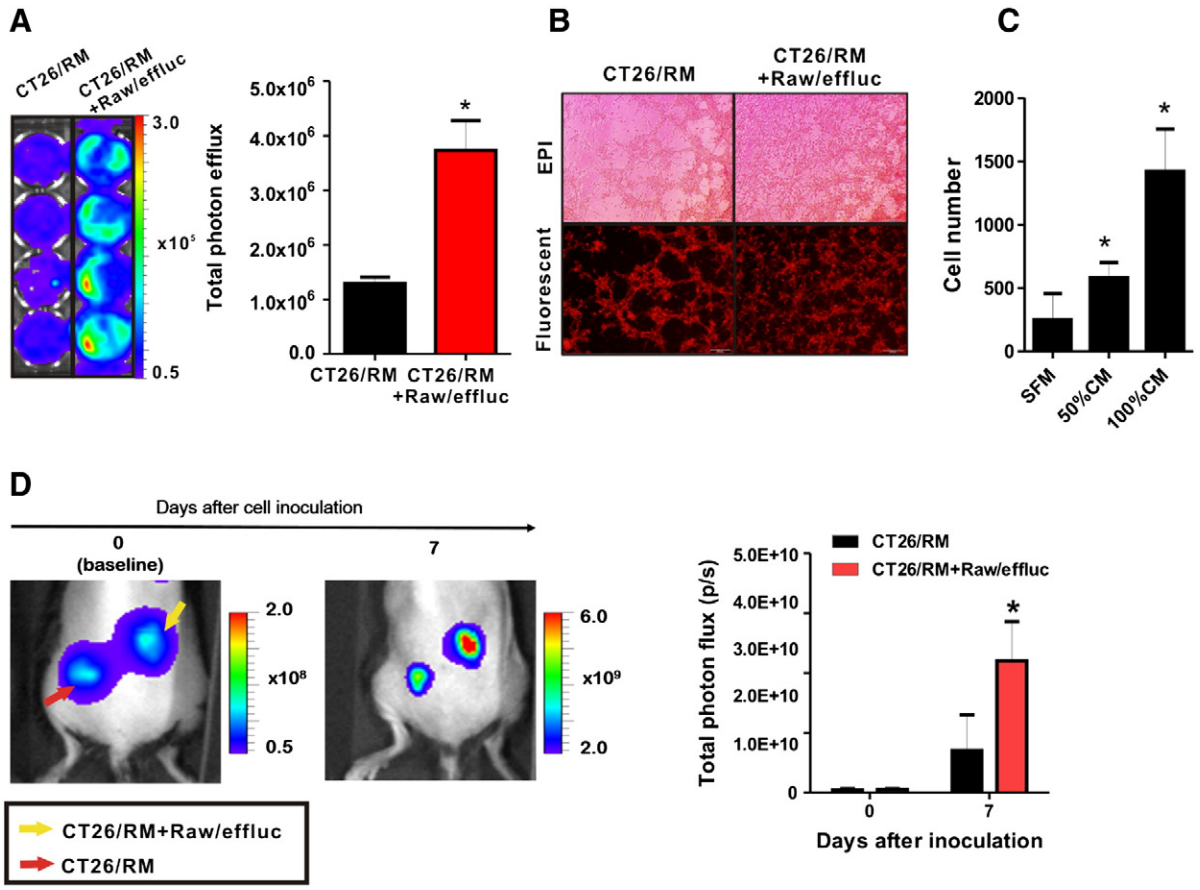

Figure 2. Evaluation of the proliferation level of colon cancer cells and the migration ability of TAMs. (A) *In vitro* BLI showing increased proliferation of CT26/RM cells by Raw/effluc cells and quantification of BLI signal. *CT26/RM versus CT26/RM+Raw/effluc. (B) Fluorescent microscopic analysis. CT26/RM cells (1×10^4 cells/well) were plated without or with Raw/effluc cells (1×10^3 cells/well). After 24 hours, BLI activity was measured with the IVIS Lumina III, and fluorescent microscope images were acquired. (C) Transwell migration assay. After the addition of Raw/effluc to the upper chamber, the migrated Raw/effluc cells to the lower chamber containing CM from CT26/RM were collected and counted by flow cytometry. *SFM versus SFM. (D) Imaging of enhanced proliferation of CT26/RM cells by Raw/effluc cells and quantification of BLI signal. CT26/RM cells (1×10^6 cells) were mixed without or with Raw/effluc cells (1×10^5 cells), and these mixtures were subcutaneously injected to predetermined sites in mice. *CT26/RM alone versus CT26/RM+Raw/effluc.

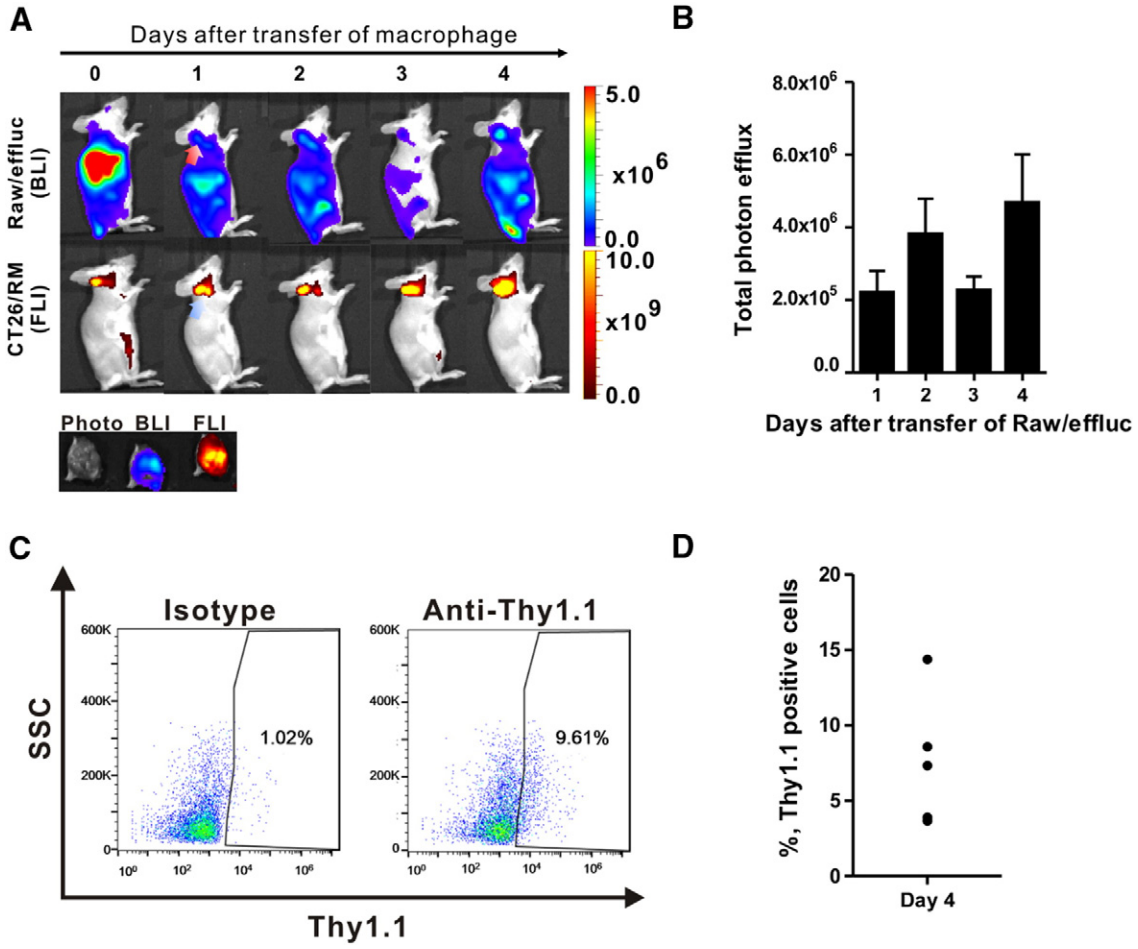

Figure 3. Visualization of TAMs migration to tumor lesion. (A) *In vivo* imaging of TAM migration to tumor lesions (inset: *ex vivo* imaging of excised tumor; left: photograph of excised tumor, middle: BLI of Raw/effluc, right: FLI of CT26/RM tumor). (B) Quantification of BLI signal. Red arrow: Migrated macrophage; blue arrow: tumor site. (C and D) Levels of Thy1.1-positive cells in isolated cells of excised tumor of mice receiving Raw/effluc cells. The isolated cells of the excised tumor were labeled with Thy1.1-specific antibody (surrogate for effluc), and the number of Thy1.1-postivie cells was determined with flow cytometry.

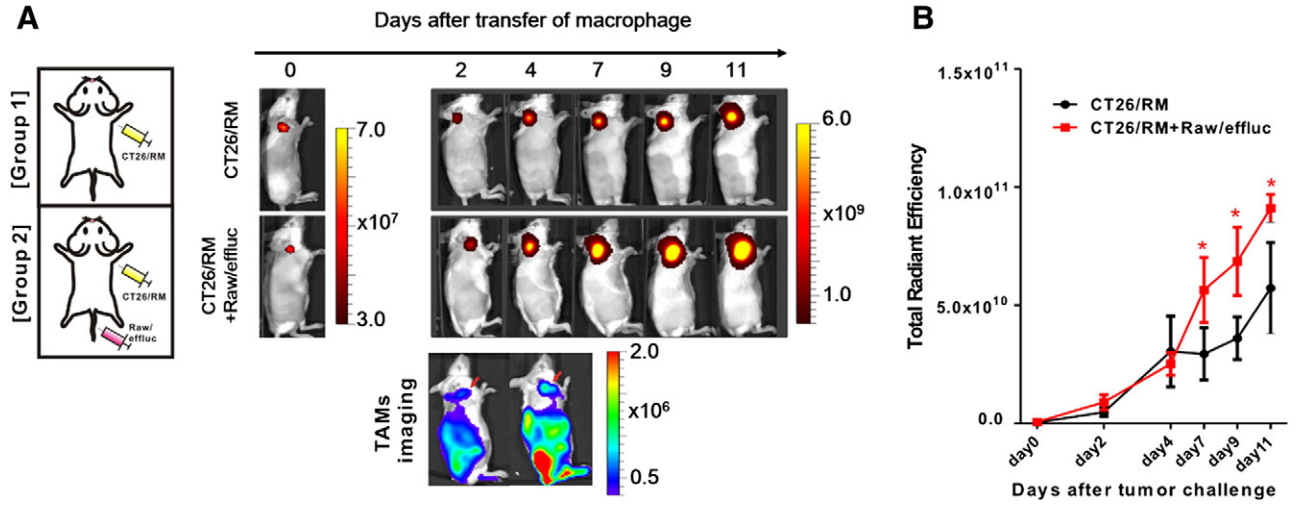

Figure 4. *In vivo* monitoring of tumor growth modulated by migrated TAMs. (A) Visualization of enhanced tumor growth by migrated TAMs with the mCherry reporter gene and (B) quantification of the mCherry signal in tumors. Tumor-bearing mice received either PBS or Raw/effluc via the tail vein, and tumor progression was monitored. The localization of infused TAMs in CT26/RM tumors is shown at days 2 and 3 posttransfer by BLI. *CT26/RM alone versus CT26/RM+Raw/effluc.

which was before the transfer of Raw/effluc cells (Figure 4*A*). Interestingly, *in vivo* FLI of tumor growth showed higher tumor growth in the CT26/RM+Raw/effluc group than in the CT26/RM-alone group. A significant difference in tumor growth was confirmed by serial imaging between day 7 and day 11 posttransfer of Raw/effluc cells (Figure 4*B*, $P < .05$). The migration of infused Raw/effluc cells to tumor lesions was also detected at days 2 and 4 posttransfer of Raw/effluc cells (see *red arrow* in Figure 4*A*).

Evaluation of the Effects of DEX on Both Macrophage Migration to Tumor Lesions and Modulated Tumor Progression with Combined BLI and FLI

Next, we examined the DEX effects on both TAM migration to tumors and modulation of tumor growth by combined BLI and FLI (Supplementary Figure S4). Treatment with DEX resulted in a significant inhibition of Raw/effluc infiltration to tumor lesions when compared with the vehicle-treated group based on *in vivo* BLI (Figure 5*A*). *In vivo* FLI of tumor growth demonstrated that the rate of tumor growth is significantly higher in the CT26/RM+Raw/effluc group than the CT26/RM alone group (Figure 5, *B* and *C*; $P < .05$). Interestingly, enhanced tumor growth via Raw/effluc cells almost completely disappeared in the DEX-treated group. The relative (%) increases in FLI signals between day 0 and day 11 (the day after the transfer of Raw/effluc cells) were 299.0 ± 72%, 539.1 ± 78.8%, and 304.8 ± 70.6% in the CT26/RM-alone, CT26/RM+Raw/effluc, and DEX-treated groups, respectively (Figure 5*D*, $P < .05$, CT26/RM+Raw/effluc group versus DEX-treated group).

Discussion

Noninvasive imaging of TAMs enabling the real-time monitoring of their distribution in tumor-bearing mice [11] is an attractive research area. It has been typically accomplished by the use of several imaging probes, such as optical imaging probes [12,13], iron oxide–based MRI probes [14], radioisotope-labeled mannose functionalized liposomes [15], and nanobodies [16]. Both MRI and nuclear imaging, or even fluorescence imaging using dye-labeled probes, have much more potential than BLI (the strategy used in this study) for clinical use. So far, BLI can only be used in preclinical studies; however, MRI and nuclear imaging are routinely used in the clinical practice.

Reporter gene-based multimodal optical imaging has been extensively investigated to simultaneously monitor the biological behavior of several cells of interest, such as immune effectors, stem cells, and cancer cells, owing to its high sensitivity, easy application, and the lack of a need for expensive facilities and complex synthesis procedures [9,10]. Using BLI, it is possible to visualize the localization, proliferation, and migration of various cells, e.g., to track tumor progression and the recruitment of immune effectors simultaneously, as different substrates are used for *in vivo* imaging of the effluc (D-luciferin) and Rluc (coelenterazine) genes. Moreover, FLI with monomeric far red fluorescent reporters, such as the mCherry and tdTomato proteins, enables the serial monitoring of the expression of genes of interest and tumor growth, without additional substrate injections, in living mice [17,18].

In the current study, we have succeeded in serial monitoring of the migration of TAMs to tumor lesions with effluc and evaluation of the effects of TAMs on tumor progression with the mCherry reporter. Subsequently, using established TAM trafficking strategies, we could observe the inhibitory effect of DEX, a potent anti-inflammatory drug, on TAM migration and its negative modulatory effects on tumor progression. Raw264.7 and CT26 cells were selected as TAMs and a colon cancer model based on their use in previous studies [19–21]. The introduction of reporter genes by retroviral or lentiviral systems enables the long-term monitoring of infused immune cells, stem cells, and cancer cells [22–24]. Thus, we established reporter gene-expressing macrophage and colon cancer cells using a retroviral or lentiviral system. Because the population levels of migrated TAMs to tumor lesion are quite less, we selected the highly sensitive reporter gene enhanced firefly luciferase, which has 10-fold to 9400-fold higher luciferase activity than firefly luciferase and can be used to visualize even just a few cells *in vivo* [25]. To monitor tumor progression with respect to migrated TAMs *in vivo*, CT26 cells were engineered to coexpress Rluc and mCherry using the lentiviral system; accordingly, both cell proliferation and tumor growth could be examined by a combination of BLI and FLI *in vitro* and *in vivo*.

TAMs promote the proliferation of cancer cells by upregulating angiogenic factors [7,8]. Consistent with these findings, both *in vitro* BLI and FLI revealed that Raw/effluc cells promoted the proliferation of CT26/RM cells. Consistent with the *in vitro* findings, *in vivo* BLI using *Rluc* showed the enhanced proliferation of CT26/RM cells when Raw/effluc cells are coinjected with CT26/RM cells. Cancer cells secrete several chemokine attractants, such as CCL2, CCL5, CCL7, CCL8, CXCL12, VEGF, and CSF-1. These promote TAM migration to tumor lesions [26]. Using a Transwell migration assay, we also found that CM as a chemoattractant from CT26/RM cells promotes the migration of Raw/effluc cells in a dose-dependent manner. These finding suggest that Raw/effluc cells have TAM characteristics and that both Raw/effluc and CT26/RM cells are suitable for *in vivo* visualization of biological behavior in tumor-bearing mice.

It has been proposed that TAMs are an important component in the tumor microenvironment and are continuously recruited to tumors via several chemoattractants, leading to a poor prognosis for several types of cancers [7]. Serial monitoring of the dynamic recruitment of TAMs is important to understand their biological role in tumor microenvironments; accordingly, we tracked TAM migration to CT26/RM tumor lesions using the effluc gene. Upon transfer of Raw/effluc cells to tumor-bearing mice, they were observed in the lung and rapidly moved to the spleen. Interestingly, on day 1 posttransfer, we detected migrated Raw/effluc cells in tumor lesions, and BLI signals were still evident at day 4. Using multimodal reporter gene-based imaging, we can find that the BLI signals of Raw/effluc cells were consistent with the FLI signals from CT26/RM. Similar with our finding, other groups have found the upregulation of numerous chemotactic cytokines and angiogenic factors including CCL2, CSF-1, VEGF, and TGF-β in CT26/DsRed cells cocultured with Raw264.7/GFP CM by the use of microarray analysis, which finally leads to the enhanced migration of Raw/GFP to CT26/DsRed *in vitro* [20]. From findings of our and other group, we may postulate that Raw/effluc is recruited to tumor lesions via chemokine attractants secreted from CT26/RM tumors following the distribution of infused Raw/effluc cells to several organs, even though the mechanism for increased migration of macrophage to tumor lesion is not completely addressed.

Several studies have shown that TAMs attracted by cancer cells respond to tumor-derived molecules, leading to the production of important growth factors and extracellular matrix enzymes and eventually stimulating tumor proliferation, angiogenesis, and the

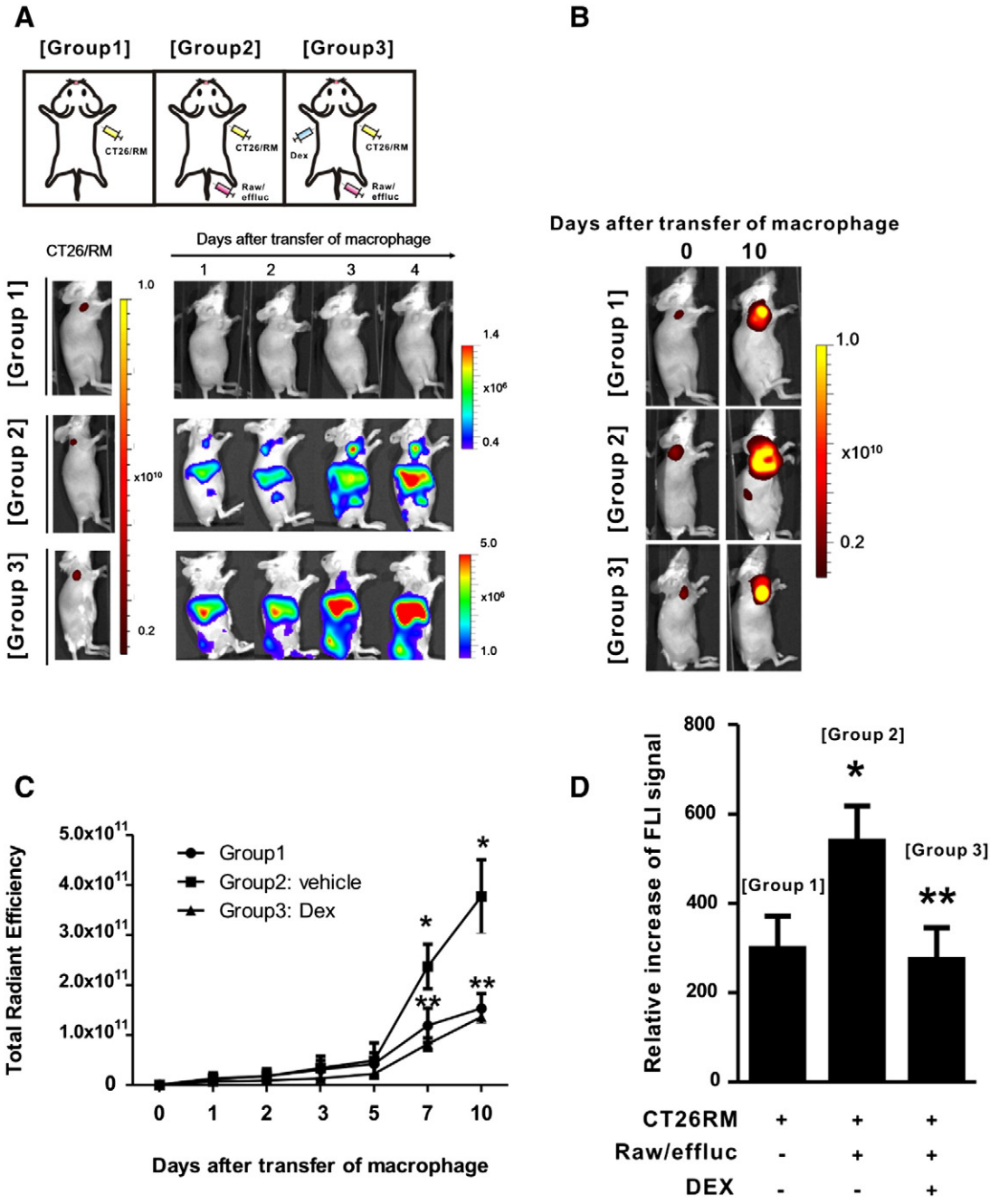

Figure 5. Evaluation of the effects of DEX on both TAM migration to tumor lesions and modulated tumor growth with BLI and FLI. (A) Inhibition of TAM migration to tumor lesions by DEX treatment. (B) Representative FLI imaging of tumor progression. (C) Quantification of mCherry signals and (D) relative increase of FLI signal in tumors. Tumor-bearing mice were divided into three groups as follows: CT26/RM alone, CT26/RM+Raw/effluc, and CT26/RM+Raw/effluc+DEX groups. Either vehicle or DEX was intraperitoneally injected to tumor-bearing mice that received Raw/effluc. BLI for TAM imaging and FLI to assess tumor growth were performed. The relative increase (%) in the signal was expressed based on a comparison between the FLI signal at day 0 and day 11. *CT26/RM versus CT26/RM+Raw/effluc, **CT26/RM+Raw/effluc versus CT26/RM+Raw/effluc+DEX.

invasion of surrounding tissues [27]. More recently, Chad et al. [20] have proven the increased expression levels of several chemotactic cytokines and angiogenic growth factors such as TGFβ, VEGF, CXCL2, and SDF-1α in Raw264.7 in response to CT26 CM by microarray analysis, which result in the enhanced proliferation and metastasis of CT26 cancer cells in *in vitro* and *in vivo* chicken egg chorioallantoic membrane assay and may induce the hindrance of killing of immune effectors like cytotoxic T lymphocyte, suggesting the positive feedback mechanism in tumor microenvironments between Raw264.7 macrophage and CT26 cancer cell. Consistent with the findings of other groups, we can successfully find that the migrated Raw/effluc cells promote tumor growth, which can be observed from day 7 posttransfer of Raw/effluc cells using multimodal reporter gene imaging.

Substantial numbers of new therapeutic reagents against TAMs that allow for their attenuation or depletion as well as the inhibition of

their migration to tumors have been developed [8,28,29]. Therefore, reliable and quantitative tools that are capable of monitoring TAM migration and evaluating the effects of TAM on tumor progression are required to investigate the therapeutic efficacy of anti-TAM candidate drugs. We evaluated the effects of DEX, which is also known as a proinflammatory cytokine inhibitor, on both TAM migration into tumor lesions and tumor growth using our established TAM imaging technique. DEX effectively regulates the expression of inflammatory cytokines [30,31] and is widely used in cancer therapy strategies [32–35]. We found that DEX effectively blocks the recruitment of TAMs to tumors and subsequently inhibits enhanced tumor growth by migrated TAMs. Although the mechanism underlying the effects of DEX on the migration of macrophage as well as the suppression of tumor growth was not fully elucidated in this study, we may postulate this phenomenon as follows: Because DEX treatment may result in the decrease of the proinflammatory cytokines at the site of tumor and in serums, the number of macrophages migrated to tumor lesion may be reduced. Subsequently, owing to DEX-induced reduction of number of macrophage migrated to tumor lesion, the level of proinflammatory cytokines in tumor microenvironment that enhance the tumor proliferation and migration will be decreased, finally leading to the suppression of promoted tumor progression. These results indicate that our TAM imaging strategy can be used to validate the efficacy of candidate drugs that modulate TAM effects in tumor microenvironments. Additionally, our results indicate that DEX has great potential for applications with conventional cancer therapies, such as chemotherapy and radiation therapy, when therapeutic efficacy is hindered by TAMs.

We should address some limitations of our current study. First, because *in vivo* tracking of TAMs migration to tumor lesion was achieved by the use of macrophage cell line, it is difficult to understand the accurate mechanism associated with TAMs migration to tumor lesion as well as their involvements in promoted tumor growth. In the future, we should focus on tracking the migration of primary TAMs in living mice. Second, we focused on only one model of tumor such as colon cancer. Next study might be conducted in other types of tumor such as breast cancer, lung cancer, etc.

Conclusion

To our knowledge, this is the first study to simultaneously evaluate the migration of TAMs to tumor lesions and the modulation of tumor progression by migrated TAMs, as well as the efficacy of an anti-TAM drug with multimodal reporter gene-based imaging in immunocompetent mice with a colon cancer model. We expect that our results will facilitate the development of new candidate drugs that attenuate TAM functions or abolish its migration into tumor lesions.

Acknowledgements

This work was supported by a National Research Foundation of Korea (NRF) grant funded by the Korean government (MSIP) (2009-0078222, 2009-0078234); a grant of the Korea Health Technology R&D Project, Ministry of Health & Welfare (HI11C1300); a grant from National Nuclear R&D Program through the NRF funded by the Ministry of Education, Science and Technology (2012M2A2A7014020); a grant from the Medical Cluster R&D Support Project through the Daegu-Gyengbuk Medical Innovation Foundation, a grant from the Ministry of Health & Welfare (HT13C0002), a grant from BK21 Plus KNU Biomedical Convergence Program, Department of Biomedical Science, Kyungpook National University; an NRF grant funded by the Korean government (MSIP) (2014R1A1A1003323); a grant from the Korea Health Technology R&D Project through the Korea Health Industry Development Institute; a grant from Basic Science Research Program through the NRF funded by the Ministry of Education, Science, and Technology (NRF-2014R1A1A2055894); a grant from the Ministry of Health & Welfare (HI15C0001); and an NRF grant funded by the Korean government (MSIP (NRF-2015M2A2A7A01045177).

Appendix A. Supplementary data

Supplementary data to this article can be found online at http://dx.doi.org/10.1016/j.neo.2016.01.004.

References

[1] Moore KJ and Tabas I (2011). Macrophages in the pathogenesis of atherosclerosis. *Cell* **145**, 341–355.
[2] McNelis JC and Olefsky JM (2014). Macrophages, immunity, and metabolic disease. *Immunity* **41**, 36–48.
[3] Bianchi ME and Manfredi AA (2014). How macrophages ring the inflammation alarm. *Proc Natl Acad Sci U S A* **111**, 2866–2867.
[4] Chawla A, Nguyen KD, and Goh YP (2011). Macrophage-mediated inflammation in metabolic disease. *Nat Rev Immunol* **11**, 738–749.
[5] Allavena P, Sica A, Solinas G, Porta C, and Mantovani A (2008). The inflammatory micro-environment in tumor progression: the role of tumor-associated macrophages. *Crit Rev Oncol Hematol* **66**, 1–9.
[6] Condeelis J and Pollard JW (2006). Macrophages: obligate partners for tumor cell migration, invasion, and metastasis. *Cell* **124**, 263–266.
[7] Pollard JW (2004). Tumour-educated macrophages promote tumour progression and metastasis. *Nat Rev Cancer* **4**, 71–78.
[8] Brower V (2012). Macrophages: cancer therapy's double-edged sword. *J Natl Cancer Inst* **104**, 649–652.
[9] Kang JH and Chung JK (2008). Molecular-genetic imaging based on reporter gene expression. *J Nucl Med* **49**(Suppl. 2), 164S–179S.
[10] Blasberg RG and Tjuvajev JG (2003). Molecular-genetic imaging: current and future perspectives. *J Clin Invest* **111**, 1620–1629.
[11] Weissleder R, Nahrendorf M, and Pittet MJ (2014). Imaging macrophages with nanoparticles. *Nat Mater* **13**, 125–138.
[12] Verdoes M, Edgington LE, Scheeren FA, Leyva M, Blum G, Weiskopf K, Bachmann MH, Ellman JA, and Bogyo M (2012). A nonpeptidic cathepsin S activity-based probe for noninvasive optical imaging of tumor-associated macrophages. *Chem Biol* **19**, 619–628.
[13] Sun X, Gao D, Gao L, Zhang C, Yu X, Jia B, Wang F, and Liu Z (2015). Molecular imaging of tumor-infiltrating macrophages in a preclinical mouse model of breast cancer. *Theranostics* **5**, 597.
[14] Daldrup-Link H and Coussens LM (2012). MR imaging of tumor-associated macrophages. *Oncoimmunology* **1**, 507–509.
[15] Locke LW, Mayo MW, Yoo AD, Williams MB, and Berr SS (2012). PET imaging of tumor associated macrophages using mannose coated 64Cu liposomes. *Biomaterials* **33**, 7785–7793.
[16] Movahedi K, Schoonooghe S, Laoui D, Houbracken I, Waelput W, Breckpot K, Bouwens L, Lahoutte T, De Baetselier P, and Raes G, et al (2012). Nanobody-based targeting of the macrophage mannose receptor for effective in vivo imaging of tumor-associated macrophages. *Cancer Res* **72**, 4165–4177.
[17] Yamaoka N, Kawasaki Y, Xu Y, Yamamoto H, Terada N, Okamura H, and Kubo S (2010). Establishment of in vivo fluorescence imaging in mouse models of malignant mesothelioma. *Int J Oncol* **37**, 273–279.
[18] Winnard Jr PT, Kluth JB, and Raman V (2006). Noninvasive optical tracking of red fluorescent protein-expressing cancer cells in a model of metastatic breast cancer. *Neoplasia* **8**, 796–806.
[19] Chen P, Huang Y, Bong R, Ding Y, Song N, Wang X, Song X, and Luo Y (2011). Tumor-associated macrophages promote angiogenesis and melanoma growth via adrenomedullin in a paracrine and autocrine manner. *Clin Cancer Res* **17**, 7230–7239.
[20] Green CE, Liu T, Montel V, Hsiao G, Lester RD, Subramaniam S, Gonias SL, and Klemke RL (2009). Chemoattractant signaling between tumor cells and macrophages regulates cancer cell migration, metastasis and neovascularization. *PLoS One* **4**, e6713.
[21] Zhang B, Wang J, Gao J, Guo Y, Chen X, Wang B, Gao J, Rao Z, and Chen Z (2009). Alternatively activated RAW264.7 macrophages enhance tumor

lymphangiogenesis in mouse lung adenocarcinoma. *J Cell Biochem* **107**, 134–143.

[22] De A, Lewis XZ, and Gambhir SS (2003). Noninvasive imaging of lentiviral-mediated reporter gene expression in living mice. *Mol Ther* **7**, 681–691.

[23] Kim HJ, Jeon YH, Kang JH, Lee YJ, Kim KI, Chung HK, Jeong JM, Lee DS, Lee MC, and Chung JK (2007). In vivo long-term imaging and radioiodine therapy by sodium-iodide symporter gene expression using a lentiviral system containing ubiquitin C promoter. *Cancer Biol Ther* **6**, 1130–1135.

[24] Gerolami R, Uch R, Jordier F, Chapel S, Bagnis C, Brechot C, and Mannoni P (2000). Gene transfer to hepatocellular carcinoma: transduction efficacy and transgene expression kinetics by using retroviral and lentiviral vectors. *Cancer Gene Ther* **7**, 1286–1292.

[25] Rabinovich BA, Ye Y, Etto T, Chen JQ, Levitsky HI, Overwijk WW, Cooper LJ, Gelovani J, and Hwu P (2008). Visualizing fewer than 10 mouse T cells with an enhanced firefly luciferase in immunocompetent mouse models of cancer. *Proc Natl Acad Sci U S A* **105**, 14342–14346.

[26] Sica A, Allavena P, and Mantovani A (2008). Cancer related inflammation: the macrophage connection. *Cancer Lett* **267**, 204–215.

[27] Qian BZ and Pollard JW (2010). Macrophage diversity enhances tumor progression and metastasis. *Cell* **141**, 39–51.

[28] Bingle L, Brown NJ, and Lewis CE (2002). The role of tumour-associated macrophages in tumour progression: implications for new anticancer therapies. *J Pathol* **196**, 254–265.

[29] De Palma M and Lewis CE (2013). Macrophage regulation of tumor responses to anticancer therapies. *Cancer Cell* **23**, 277–286.

[30] Yang YH, Morand EF, Getting SJ, Paul-Clark M, Liu DL, Yona S, Hannon R, Buckingham JC, Perretti M, and Flower RJ (2004). Modulation of inflammation and response to dexamethasone by Annexin 1 in antigen-induced arthritis. *Arthritis Rheum* **50**, 976–984.

[31] Rhen T and Cidlowski JA (2005). Antiinflammatory action of glucocorticoids—new mechanisms for old drugs. *N Engl J Med* **353**, 1711–1723.

[32] Goulding NJ (2004). The molecular complexity of glucocorticoid actions in inflammation—a four-ring circus. *Curr Opin Pharmacol* **4**, 629–636.

[33] Ovali E, Ozdemir F, Aydin F, Kavgaci H, Tekelioglu Y, Buyukcelik A, and Yilmaz M (2003). The effects of dexamethasone on leukemic cells derived from patients with AML. *J Exp Clin Cancer Res* **22**, 85–89.

[34] Piette C, Deprez M, Roger T, Noel A, Foidart JM, and Munaut C (2009). The dexamethasone-induced inhibition of proliferation, migration, and invasion in glioma cell lines is antagonized by macrophage migration inhibitory factor (MIF) and can be enhanced by specific MIF inhibitors. *J Biol Chem* **284**, 32483–32492.

[35] Shiratsuchi T, Ishibashi H, and Shirasuna K (2002). Inhibition of epidermal growth factor–induced invasion by dexamethasone and AP-1 decoy in human squamous cell carcinoma cell lines. *J Cell Physiol* **193**, 340–348.